Water as probe molecule for midgap states in nanocrystalline strontium titanate by conventional and synchronous luminescence spectroscopy under ambient conditions

Sean Taylor, Alexander Samokhvalov *

Chemistry Department, Rutgers University, 315 Penn St., Camden, NJ 08102, USA

ABSTRACT

Alkaline earth metal titanates are broad bandgap semiconductors with applications in electronic devices, as catalysts, photocatalysts, sorbents, and sensors. Strontium titanate $SrTiO_3$ is of interest in electronic devices, sensors, in the photocatalytic hydrogen generation, as catalyst and sorbent. Both photocatalysis and operation of electronic devices rely upon the pathways of relaxation of excited charge in the semiconductor, including relaxation through the midgap states. We report characterization of nanocrystalline $SrTiO_3$ at room temperature by "conventional" vs. synchronous luminescence spectroscopy and complementary methods. We determined energies of radiative transitions in the visible range through the two midgap states in the nanocrystalline $SrTiO_3$. Further, adsorption and desorption of vapor of water as "probe molecule" for midgap states in the nanocrystalline $SrTiO_3$ was studied, for the first time, by luminescence spectroscopy under ambient conditions. Emission of visible light from the nanocrystalline $SrTiO_3$ is significantly increased upon desorption of water and decreased (quenched) upon adsorption of water vapor, due to interactions with the surface midgap states.

© 2016 Elsevier B.V. All rights reserved.

1. Introduction

Strontium titanate $SrTiO_3$ is a broad bandgap semiconductor which has been studied as a photocatalyst [1], catalyst [2], sorbent [3], material in electronic devices [4] and gas sensors [5]. Above 106 K including the room temperature, $SrTiO_3$ is present in distorted cubic perovskite structure [6]. For the single crystals of $SrTiO_3$, the energy is 3.75 eV for a direct bandgap and 3.25 eV for an indirect bandgap [7]. Electronic midgap states play an important role in modulation of optical absorption in semiconductors [8] and in charge transport, in particular as charge-trapping centers which affect photoconductivity [9] and photocatalytic reaction rates [10].

The photoluminescence (PL) spectroscopy is well suited for characterization of electronic states in powdered semiconductors [11] including metal oxides [12], zeolites [13,14], etc. The "conventional" PL emission spectrum is obtained by recording the emission wavelength λ_{emiss} under photoexcitation at a constant λ_{exc}. The PL excitation spectrum is collected by changing λ_{exc} while the emission is recorded at a constant λ_{emiss}. The narrower emission spectra can be obtained by using synchronous luminescence spectroscopy [15] in which the λ_{exc} and λ_{emiss} are changed simultaneously at a constant difference $\Delta\lambda = \lambda_{emiss} - \lambda_{exc}$. Applications of synchronous fluorescence spectroscopy

have recently been reviewed [16,17]. Synchronous luminescence spectroscopy has not been reported in characterization of nanocrystalline strontium titanate, to our knowledge.

Adsorption based applications frequently involve moisture in ambient air, so this is important to study mechanisms of adsorption of water in the vapor phase. The water molecule has a high energy of stretching vibration at ca. 3500 cm^{-1}, and water has been studied as a "probe molecule" in the PL quenching experiments with chemical compounds of several classes. These include inorganic ions in solution [18], metal-organic frameworks [19], semiconductor nanoparticles with lanthanide metal dopants [20–22] as well as without dopant such as CdS [23] and PbS [24].

Recently, we used the PL spectroscopy to study emission from monomers and excimers of molecules of aromatic hydrocarbons [25] and aromatic sulfur compounds [26]. We also applied the in-situ PL spectroscopy to learn about the direction of transfer of photoexcited charge in photocatalytic colloids of metal-doped titanium dioxide [27] and the ex-situ PL spectroscopy to study radiative transitions in the nanocrystalline binary nitrogen and metal codoped titanium dioxide [28]. Recently, we compared the "conventional" and synchronous luminescence spectra of the nanocrystalline calcium titanate with orthorhombic lattice measured at 77 K inside a liquid nitrogen Dewar [29]. In this work, we study water in the vapor phase as the universal spectroscopic "probe molecule" interacting with electronic midgap states in the nanocrystalline $SrTiO_3$ with cubic lattice under ambient conditions. Reversible adsorption/desorption of water causes a reversible quenching/

* Corresponding author at: Department of Chemistry, Rutgers University, Camden, NJ 08102, USA.

E-mail address: alexsam@camden.rutgers.edu (A. Samokhvalov).

increase of the photoluminescence in the visible range originating from the midgap states in $SrTiO_3$. We characterize midgap states in the nanocrystalline $SrTiO_3$ by synchronous luminescence spectroscopy at a convenient temperature of 25 °C versus "conventional" PL emission spectroscopy, and by the complementary methods. In addition, we determine the pathways of relaxation of excited charge in the nanocrystalline cubic $SrTiO_3$ through the midgap electronic states.

2. Materials and Methods

2.1. Materials

Nanopowder of $SrTiO_3$ (99.95% purity, <100 nm nominal particle size, cubic phase) has been obtained from the U.S. Research Nanomaterials. Sulfuric acid and hydrogen peroxide were from Fisher.

2.2. Specimen Characterization

XRD data were obtained using Rigaku SmartLab diffractometer system with Cu K-alpha line at 0.15418 nm. The Raman spectra were collected at room temperature with XploRA confocal microscope from Horiba Scientific which is equipped with lasers at 532 nm, 638 nm and 785 nm, and has a cut-off filter at 50 cm^{-1}. The UV–Visible diffuse reflectance spectra, UV–Vis DRS were measured at room temperature with Cary 5000 spectrometer equipped with Praying Mantis attachment from Harrick Scientific. As white reference, finely grinded $BaSO_4$ of 99.998% purity from Alfa Aesar has been used.

2.3. Drying and Hydration of $SrTiO_3$

The as-obtained $SrTiO_3$ nanopowder denoted asisSrTiO$_3$ was dried at 105 °C in the oven overnight, yielding dried material drSrTiO$_3$. The drSrTiO$_3$ was hydrated using the procedure recently reported by us [19], by being placed inside the desiccator with liquid water and kept in contact with water vapor at relative humidity RH ~ 100% at 25 °C overnight, resulting in hydrated material hydSrTiO$_3$.

2.4. Measurements by the Photoluminescence (PL) Spectroscopy

All spectra were recorded using Fluorolog spectrometer FL3-22 from Horiba Scientific. This instrument is equipped with dual monochromator gratings on the excitation and emission optical pathways. In order to minimize artifacts due to primary and secondary re-absorption of light in solids [30], all spectra were collected in the Front Face (FF) geometry using FL-1001 accessory from Horiba Scientific. In addition, to avoid the effects of fluctuations in the intensity of the excitation light source on the spectra, the signal from the sample (S1) has been divided by the reference signal (R1) generated by the excitation beam before reaching the sample, and the ratio S1/R1 has been utilized in all cases.

The 0.5 cm^3 quartz cuvette was cleaned with Piranha solution (sulfuric acid and hydrogen peroxide), rinsed with distilled water, and dried. All PL measurements were conducted at 25 °C, with the sample placed into a freshly cleaned and dried 0.5 cm^3 quartz cuvette, closed with polytetrafluoroethylene (PTFE) stopper, and sealed with Parafilm tape to exclude ambient moisture. The temperature of the sample in the cavity of the spectrometer was maintained at 25 °C by water circulation thermostat model A25 from Thermo Scientific. The PL emission spectra were collected at the excitation and emission optical slits at 2 nm. The excitation wavelength λ_{exc} has been varied from 250 nm (an extra bandgap excitation in $SrTiO_3$) to 460 nm (the sub bandgap excitation) in steps of 10 nm. In synchronous luminescence spectroscopy, the $\Delta\lambda$ parameter has been changed from $\Delta\lambda = 10$ nm to $\Delta\lambda = 120$ nm. Numeric fitting of the spectra was performed with Microcal Origin 2015 program.
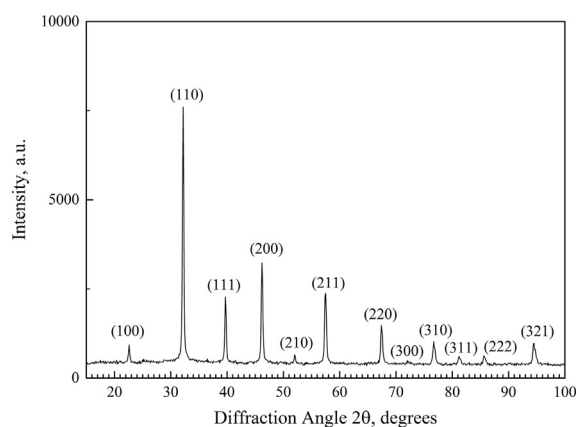

Fig. 1. XRD pattern of nanocrystalline $SrTiO_3$.

3. Results and Discussion

3.1. Structural Characterization of Nanocrystalline $SrTiO_3$

Fig. 1 shows an XRD pattern of our nanocrystalline $SrTiO_3$; the peaks correspond to the perovskite phase, they can be indexed to the cubic space group, and the pattern matches the PDF card # 01-089-4934 (tausonite). The cubic lattice of our nanocrystalline $SrTiO_3$ is also consistent with the JCPDS card # 05-0634 of cubic perovskite in previous reports [31,32]. No splitting of the (100), (110), and (200) reflections was observed which indicates an absence of a tetragonal distortion of cubic lattice. We analyzed the strongest (110) diffraction peak of our $SrTiO_3$ at $2\theta = 32.20$ deg. by the Scherrer's equation [33], $D = k\,\lambda\,/\,\beta\cos(\theta)$, where k is a constant (the shape factor with numeric value of 0.9), λ is an X-ray wavelength, β is the full-width at half-maximum (FWHM) of the diffraction peak of interest (in radian), and θ is the Bragg angle. This analysis yields the average nanocrystalline size of our nanocrystalline $SrTiO_3$ at 36 nm.

Fig. S1 shows the Raman spectrum of nanocrystalline $SrTiO_3$ at room temperature at $\lambda_{exc} = 532$ nm; the Raman spectrum at $\lambda_{exc} = 638$ nm was similar (data not shown). The Raman spectrum in Fig. S1 is consistent with published spectrum [32] of nanocrystalline cubic strontium titanate. For cubic $SrTiO_3$ of space group Pm3m, the phonons are represented by the symmetry $3F_{1u} + F_{2u}$, and neither represents the first order Raman-active mode, since the center of symmetry results in the zero polarizability of the lattice [32,34]. Assignments of the Raman peaks of our nanocrystalline $SrTiO_3$ (Fig. S1) are provided in Table 1.

Recent reports showed that vibrational modes can be modified due to electrostatic forces, oxygen vacancies and external factors, so that the F_{1u} mode is divided into a doubly degenerate E and a nondegenerate A_1 modes, while the F_{2u} mode is divided into E and B_1 modes [32]. The long-range electrostatic forces separate the degenerate mode E and the nondegenerate mode A_1 into the transverse optical (TO) and longitudinal optical (LO) modes, which are observed in the Raman spectra of strontium titanate at room temperature [34].

Table 1
Raman peaks of nanocrystalline cubic $SrTiO_3$ with assignments.

The Raman shift, cm^{-1}	The Raman shift in Ref. [32], cm^{-1}	Vibrational mode in Ref. [32]
$v_1 = 185$	179	TO2 (transverse optical)
$v_2 = 275$	270	TO3 (transverse optical)
$v_3 = 550$	544	TO4 (transverse optical)
$v_4 = 731$	727	TO (transverse optical)
$v_5 = 805$	801	LO4 (longitudinal optical)